Supplemental data

Loss of intestinal core 1–derived *O*-glycans causes spontaneous colitis in mice

Jianxin Fu[1,2*], Bo Wei[3*], Two Wen[1*], Malin E.V. Johansson[4], Xiaowei Liu[1#], Emily Bradford[5], Kristina A. Thomsson[4], Samuel McGee[1], Lilah Mansour[6], Maomeng Tong[3], Michael McDaniel[1], Thomas J. Sferra[6,7], Jerrold R. Turner[5], Hong Chen[1,7], Gunnar C. Hansson[4], Jonathan Braun[3], Lijun Xia[1,2,7]

[1]Cardiovascular Biology Research Program, Oklahoma Medical Research Foundation, Oklahoma City, OK 73104, USA. [2]Soochow University, Suzhou, 215006, China. [3]Department of Pathology and Laboratory Medicine, David Geffen School of Medicine, University of California, Los Angeles, CA 90095, USA. [4]Department of Medical Biochemistry, University of Gothenburg, Medicinaregatan 9A 413 90, Gothenburg, Sweden. [5]Department of Pathology, The University of Chicago, 5841 South Maryland, MC 1089, Chicago, IL 60637, USA. [6]Department of Pediatrics, and [7]Department of Biochemistry and Molecular Biology and Oklahoma Center for Medical Glycobiology, University of Oklahoma Health Sciences Center, Oklahoma City, OK 73104, USA

*Equal contributions

Character count:

#Current address: Second Xiangya Hospital, Central South University, Changsha, Hunan 410011, China

The authors have declared that no conflict-of-interest exists.

Correspondence:

Lijun Xia, Cardiovascular Biology Research Program, Oklahoma Medical Research Foundation, 825 N.E. 13th Street, Oklahoma City, OK 73104; Tel: (405) 271-7892; FAX: (405) 271-3137; e-mail: lijun-Xia@omrf.org

Methods

Carbohydrate stains and O-glycan structural analysis. Deparaffinized sections (5 μm thick) were stained with Alcian blue (pH 2.5; Newcomer Supply) to reveal the general carbohydrate moieties. Mucus scraped from the mouse intestine was extracted in 6 M guanidinium chloride supplemented with protease inhibitors (2× Complete protease inhibitor mix; Roche) (1, 2), stirred overnight at 4°C and centrifuged for 20 min at 16,000 ×*g*. Extractions were repeated three times. The samples were reduced in guanidine hydrochloride with DTT (100 mM) at 37°C for 3 h and alkylated with iodoacetamide (250 mM) overnight. The samples were dialyzed against water and solubilized in sample buffer.

Glycan analysis was done according to published methods (2). Briefly, mucins were analyzed with agarose–polyacrylamide gel electrophoresis (AgPAGE), containing agarose (0.5–1% gradient), acrylamide (0–6%), and glycerol (0–10%) on ice at 4°C with 30 mA/gel for 3 h. Separated mucins were then wet-blotted to PVDF membranes. The mucin bands were visualized with Alcian blue, and oligosaccharides were released from the blot as alditols with reductive beta elimination (0.5 M $NaBH_4$ in 50 mM KOH) at 50°C overnight. The samples were neutralized and desalted, followed by repeated evaporation of borate. The oligosaccharides were analyzed with reversed-phase liquid chromatography/mass spectrometry using a gradient with 8 mM NH_4HCO_3 and acetonitrile. The HPLC columns (10 cm × 250 μm, i.d.) were graphitized carbon (Hypercarb) and were packed in-house. The mass spectrometer was an LTQ linear quadrupole ion trap mass spectrometer (Thermo Electron) operating in negative mode. MS/MS experiments were performed on the three most abundant ions in each full scan. The spectra were evaluated manually.

Mucin gene expression. Total RNA was prepared from colons with TRIzol reagent (Invitrogen) and treated with DNase I (Ambion). cDNA was synthesized from 2 μg total RNA using M-MLV reverse transcriptase (Invitrogen) and oligo(dT) primers. Real-time PCR was performed on an ABI Prism 7000

spectrofluorometric thermal cycler (Applied Biosystems) using SYBR-green as a double-stranded DNA–specific binding dye. 18s rRNA was used to normalize the amount and quality of the RNA. The primers used are Muc1: 5'-CCAGACCCCTGCACTCTGAT-3' and 5'-CGCTTGACAAAGGGCATGA-3'; Muc2: 5'-TGCCCACCTCCTCAAAGAC-3' and 5'-TAGTTTCCGTTGGAACAGTGAA-3'; Muc3: 5'-GTGGGACGGGCTCAAATG-3' and 5'-CTGTGTGTTGGCAATTTCTG-3'; Muc4: 5'-CAATGCCCTCCACAAAAAGT-3' and 5'-CTGTGTGTTGGCAATTTCTG-3' and Muc5ac: 5'-TGGTTTGACACTGACTTCCC-3' and 5'-TCCTCTCGGTGACAGAGTCT-3'.

Flow cytometry. Single-cell suspensions were obtained by passing the spleen or mesenteric lymph node through a 100-μm cell strainer. Red blood cells were lysed by a 15-min incubation in ammonium chloride lysing reagent (BD Biosciences). Intestinal intraepithelial lymphocytes from colons were isolated as described(3). All antibodies were obtained from BD Biosciences unless specified otherwise. For myeloid cell analysis, peripheral blood leukocytes that were positive for myeloid marker CD11b but negative for the rest of the lineage markers were defined as monocytes (4). mAb against Ly-6C (AL-21) was used to classify monocytes into subsets with either high expression of Ly-6C (Ly-6C^{hi}) or low expression of Ly-6C (Ly-6C^{lo}). Cells from indicated compartments were incubated with antibodies. Two-color analyses were performed using the FACSCalibur system (BD Biosciences).

Detection of non-O-glycosylated Muc2 precursor in the ER. All mucin-type O-glycosylation steps occur in the Golgi (5). Therefore, the non-O-glycosylated precursor form of O-glycoproteins such as mucins can only be detected in the ER. To determine whether lack of core 1-derived *O*-glycans causes abnormal accumulation of Muc2 in the ER, cryosections of WT or IEC *C1galt1*$^{-/-}$ colon tissues (12 weeks old) were stained with FITC-labeled anti-Muc2 Gpda antiserum (PH497) that specifically recognizes non-O-glycosylated Muc2 precursor in the ER (6). Sections were mounted in ProLong Gold antifade (Invitrogen). Pictures were obtained with a Radiance 2000 (Bio-Rad) confocal microscope.

Detection of XBP1 transcripts by RT-PCR. Total RNA was isolated from distal colons of WT and

TM-IEC *C1galt1*$^{-/-}$ mice 15 days after TM injection. Reverse transcripition (RT) was carried out with 2 μg RNA using oligo(dT) primers. PCR using forward primer: 5'-GAA CCA GGA GTT AAG AAC ACG-3' and reverse primer: 5'-AGG CAA CAGTGT CAG AGT CC-3' was performed to detect the unspliced and spliced isoforms of XBP1 (7). RNA from mouse type 1 astrocytes treated with or without tunicamycin (10 ug/ml for 14 h; Sigma), which inhibits N-linked glycosylation and subsequently induces UPR (7), was used as positive or negative control, respectively.

Anti-C3GnT staining. For the experiment, deparaffinized sections were firstly treated for 15 min with 20 ug/ml proteinase K (Roche) for antigen retrieval, and then incubated with a strepavidin/biotin blocking kit (Dako) as well as 3% H_2O_2 for blocking endogenous peroxidase activity. Sections were subsequently blocked for nonspecific antibody binding using a protein blocking kit (Dako). Sections were incubated overnight at 4°C with rabbit anti-C3GnT antibody (1:100; Sigma-Aldrich), or with an isotype-matched control rabbit IgG. The sections were finally incubated with biotinylated goat anti-rabbit secondary antibody (Vector Laboratories) and followed by an incubation of HRP-streptavidin (Vector Laboratories), and then developed with a diaminobenzidine substrate and counterstained with hemotoxylin.

C1GALT1C1 mutation analysis. To identify whether mutations in *C1GALT1C1* cause the Tn expression we observed in patient samples, we collected the Tn-positive epithelial cells from paraffin biopsy sections after Tn staining using the Arcturus PixCell Laser Capture Microdissection instrument (Molecular Devices). Tn-negative cells from the same sample were collected as controls. Genomic DNA was extracted from these samples using a micro-DNA isolation kit (Qiagen), and PCR was performed using the Phusion High-Fidelity PCR kit (New England Biolabs) with primers as indicated (Supplemental Figure 10A). *C1GALT1C1* has a single coding exon; therefore, we were able to design PCR primers that amplified the entire *C1GALT1C1* coding region (8). The open reading frame of *C1GALT1C1* was amplified with high-fidelity PCR (Agilent) using human *C1GALT1C1*–specific

primers (forward, 5'-CTCCATAGAGGAGTTGTTGC-3'; reverse, 5'-TCACGCTTTTCTACCACTTC-3') and directly sequenced.

Results and discussion

The expression of core 3 β1,3-N-acetylglucosaminyltransferase (C3GnT) is not altered in UC colon samples. *O*-glycans are synthesized post-translationally in the Golgi apparatus through a series of sequential reactions catalyzed by specific glycosyltransferases (9-12). The primary structure of *O*-glycans is referred to as Tn antigen (GalNAcα-O-Ser/Thr), and Tn antigen is the only structure common to all *O*-glycans (Figure 1A). Tn antigen is normally modified by additional glycosylation to form two subtypes classified as core 1- and core 3-derived structures (Figure 1A) (3, 11). Core 1 *O*-glycans are the predominant form of *O*-glycans that are present in most tissues and are especially plentiful in endothelial cells, epithelial cells, and hematopoietic cells (11). Core 1 is formed through the addition of galactose (Gal) to the N-acetylgalactosamine (GalNAc) by the enzyme core 1 β1,3-galactosyltransferase (C1galt1, T-synthase) (11, 13). The production of the core 3 *O*-glycans is controlled by core 3 β1,3-N-acetylglucosaminyltransferase (C3GnT), which uses the same GalNAca-Ser/Thr substrate as T-synthase (3, 14). The expression of core 3 O-glycans is restricted to the colon and salivary glands (3).

By staining archived colon biopsy samples from ulcerative colitis (UC) patients and from normal controls (biopsy was performed for medical reasons other than IBD) with anti-Tn, we found nearly 17% (8 out of 46) UC samples were Tn-positive (Figure 6), whereas all control samples were negative. Tn antigen is a biosynthetic intermediate in the formation of normal mucin-type *O*-glycans and is typically extended by the actions of C3GnT or C1galt1 (Figure 1A). Therefore, the exposure of the Tn antigen could be resulted from defective biosynthesis of either core 1 or core 3 *O*-glycans. To test whether the biosynthesis of core 3 is abnormal, we examined the expression of C3GnT in colon biopsy

samples from UC and normal controls by immunohistochemical staining. The anti-C3GnT staining detected no significant changes in C3GnT expression in 46 UC samples compared to that in 11 normal control samples (Supplemental Figure 10). These results indicate that the expression of Tn in some UC samples is not caused by impaired biosyntheis of core 3 *O*-glycans.

Tn-antigen positive colon epithelial cells from patients with UC contain mutated C1GALT1C1. So far, no mutation of human *C1galt1* has been found. Somatic mutations in *C1GALT1C1*, the molecular chaperone specific for *C1galt1* have, however, been reported (15). *C1GALT1C1* is located on the X chromosome. This increases the likelihood that a somatic mutation in this gene will lead to a phenotypic alteration. We used genomic DNA isolated from epithelial cells of paraffin biopsy sections of UC patients after Tn staining to detect whether *C1GALT1C1* mutations occur in the Tn-positive cells. Because of limited epithelial cells from each biopsy sample and the way the samples were preserved (formalin fixed and paraffin embedded), *C1GALT1C1* products were amplified by PCR from only three of the eight Tn-positive UC samples (Supplemental Figure 11A). PCR products were sequenced directly with two sets of forward and reverse primers and also cloned into the TOPO blunt-end cloning vector (Invitrogen) for additional confirmation sequencing. Sequences verified by both forward and reverse sets of primers were used for analysis. The direct PCR products contained *C1GALT1C1* from Tn-positive and contaminating Tn-negative cells. Therefore, direct sequencing of PCR products from samples with *C1GALT1C1* mutations showed both normal and mutated nucleotides of *C1GALT1C1*. Out of the three Tn-positive UC samples, we identified four mutations. The sequencing results were confirmed with independent PCR products and verified after cloning the PCR products into the pCR4 vector. Interestingly, *C1GALT1C1* from one patient (case #21) contained three mutations, all of which altered amino acid coding (Supplemental Figure 11B and C, and data not shown**)**. Sequencing of PCR products amplified from independently collected Tn-positive crypt samples from the same patient reproduced the same result, indicating that the mutations were not artifacts.

To determine whether these mutations result in loss-of-function of *C1GALT1C1* as a molecular chaperone for C1galt1, we made two mutant constructs (Mut I, C-to-F mutation at 677; Mut III, G-to-T at 557, G-to-T at 677, and G-to-T at 718) based on mutations detected in UC patient #21 (Supplemental Figure 11D). Mut I was constructed using the QuikChange II site-directed mutagenesis kit (Stratagene). Mut III was generated with the *C1GALT1C1*-coding DNA sequence amplified from the Tn-positive colon epithelium of the UC patient #21 that contained three mutations. The constructs with mutant *C1GALT1C1* and with WT *C1GALT1C1* were transfected into Jurkat cells, which lacking C1galt1 activity because of loss-of-function mutations in *C1GALT1C1*(8). After G418 selection, transfected Jurkat cells were stained with anti–Tn antigen (5 μg/ml) and analyzed by flow cytometry. Cells transfected with empty pcDNA 3.1 (+) vector were used as controls. The expression of mRNA of the WT or mutant *C1GALT1C1* constructs in transfected Jurkat cells was confirmed by RT-PCR and by direct sequencing (Supplemental Figure 11A, E and data not shown). Jurkat cells transfected with empty vector (pcDNA3.1) had strong expression of Tn antigen (Supplemental Figure 11F). Expression of WT *C1GALT1C1* in Jurkat cells caused a substantial decrease in Tn antigen expression, demonstrating restored activity of C1galt1. In contrast, Tn expression in cells transfected with either Mut I or Mut III remained unchanged. This indicates that mutations identified in UC patient #21 resulted in impaired function in *C1GALT1C1*. Although the sample size in this pilot study was small, the promising results support our hypothesis that, at least in a subset of UC patients, somatic mutations of *Cosmc* can cause abnormal O-glycosylation such as expression of Tn antigen. It is necessary to continue this investigation, adding additional patient samples, especially frozen samples, to validate and improve the statistical power of this observation.

Reference:

1. Karlsson, N.G., Herrmann, A., Karlsson, H., Johansson, M.E., Carlstedt, I., and Hansson, G.C. The glycosylation of rat intestinal Muc2 mucin varies between rat strains and the small and

large intestine. A study of O-linked oligosaccharides by a mass spectrometric approach. *J Biol Chem*. 1997;272:27025-27034.
2. Andersch-Bjorkman, Y., Thomsson, K.A., Holmen Larsson, J.M., Ekerhovd, E., and Hansson, G.C. Large scale identification of proteins, mucins, and their O-glycosylation in the endocervical mucus during the menstrual cycle. *Mol Cell Proteomics*. 2007;6:708-716.
3. An, G., Wei, B., Xia, B., McDaniel, J.M., Ju, T., Cummings, R.D., Braun, J., and Xia, L. Increased susceptibility to colitis and colorectal tumors in mice lacking core 3-derived O-glycans. *J Exp Med*. 2007;204:1417-1429.
4. An, G., Wang, H., Tang, R., Yago, T., McDaniel, J.M., McGee, S., Huo, Y., and Xia, L. P-Selectin Glycoprotein Ligand-1 Is Highly Expressed on Ly-6Chi Monocytes and a Major Determinant for Ly-6Chi Monocyte Recruitment to Sites of Atherosclerosis in Mice. *Circulation*. 2008;117:3227-37
5. Tarp, M.A., and Clausen, H. Mucin-type O-glycosylation and its potential use in drug and vaccine development. *Biochim Biophys Acta*. 2008;1780:546-563.
6. Hansson, G.C., Baeckstrom, D., Carlstedt, I., and Klinga-Levan, K. Molecular cloning of a cDNA coding for a region of an apoprotein from the 'insoluble' mucin complex of rat small intestine. *Biochem Biophys Res Commun*. 1994;198:181-190.
7. Samali, A., Fitzgerald, U., Deegan, S., and Gupta, S. Methods for monitoring endoplasmic reticulum stress and the unfolded protein response. [published online ahead of print October 12, 2009]. *Int J Cell Biol.* doi:10.1155/2010/83037.
8. Ju, T., and Cummings, R.D. A unique molecular chaperone Cosmc required for activity of the mammalian core 1 beta 3-galactosyltransferase. *Proc Natl Acad Sci U S A*. 2002;99:16613-16618.
9. Ju, T., Brewer, K., D'Souza, A., Cummings, R.D., and Canfield, W.M. Cloning and expression of human core 1 beta1,3-galactosyltransferase. *J Biol Chem*. 2002;277:178-186.
10. Fu, J., Gerhardt, H., McDaniel, J.M., Xia, B., Liu, X., Ivanciu, L., Ny, A., Hermans, K., Silasi-Mansat, R., McGee, S., et al. Endothelial cell O-glycan deficiency causes blood/lymphatic misconnections and consequent fatty liver disease in mice. *J Clin Invest*. 2008;118:3725-3737.
11. Xia, L., Ju, T., Westmuckett, A., An, G., Ivanciu, L., McDaniel, J.M., Lupu, F., Cummings, R.D., and McEver, R.P. Defective angiogenesis and fatal embryonic hemorrhage in mice lacking core 1-derived O-glycans. *J Cell Biol*. 2004;164:451-459.
12. Brockhausen, I. Mucin-type O-glycans in human colon and breast cancer: glycodynamics and functions. *EMBO Rep*. 2006;7:599-604.
13. Ju, T., Cummings, R.D., and Canfield, W.M. Purification, characterization, and subunit structure of rat core 1 Beta1,3-galactosyltransferase. *J Biol Chem*. 2002;277:169-177.
14. Iwai, T., Inaba, N., Naundorf, A., Zhang, Y., Gotoh, M., Iwasaki, H., Kudo, T., Togayachi, A., Ishizuka, Y., Nakanishi, H., et al. Molecular cloning and characterization of a novel UDP-GlcNAc:GalNAc-peptide beta1,3-N-acetylglucosaminyltransferase (beta 3Gn-T6), an enzyme synthesizing the core 3 structure of O-glycans. *J Biol Chem*. 2002;277:12802-12809.
15. Ju, T., Lanneau, G.S., Gautam, T., Wang, Y., Xia, B., Stowell, S.R., Willard, M.T., Wang, W., Xia, J.Y., Zuna, R.E., et al. Human tumor antigens Tn and sialyl Tn arise from mutations in Cosmc. *Cancer Res*. 2008;68:1636-1646.

Supplemental Figure 1. Deletion of *C1galt1* abolishes the expression of core 1–derived *O*-glycans.

Reversed-phase HPLC/mass spectrometry (LC-MS) profiling of Muc2 *O*-glycans purified from WT

and IEC *C1galt1*$^{-/-}$ colon mucus. Red boxes indicate core 1–derived *O*-glycans, which were undetectable in the IEC *C1galt1*$^{-/-}$ colon sample. Blue lines mark core 3-derived *O*-glycans that were seen in both WT and IEC *C1galt1*$^{-/-}$ colon samples. Numbers represent calculated mass (*m*/*z*).

Supplemental Figure 2. IEC *C1galt1*$^{-/-}$ small intestine does not have significant inflammation. (**A**) Immunohistochemical staining of intestinal tissue sections of WT and IEC *C1galt1*$^{-/-}$ mice with anti–Tn antigen. Brown color indicates antibody binding. Scale bars, 100 μm. (**B**) H&E-stained WT and IEC *C1galt1*$^{-/-}$ ileums at different ages. Scale bars, 100 μm.

Supplemental Figure 3. Immune profiles of IEC *C1galt1*$^{-/-}$ mice. (**A**) Peripheral blood cell profiles of 4-week-old IEC *C1galt1*$^{-/-}$ mice. (**B**) Representative flow cytometry results of immune cells from different immune compartments of WT and IEC *C1galt1*$^{-/-}$ mice at 2.5 weeks old. IEL, intra-epithelial lymphocytes. CD4 and CD8, mAbs specific for these lymphocyte markers. DX-5, mAb specific for natural killer cells. F4/80, mAb specific for macrophages. (**C**) Serum cytokines of 2.5-week-old mice.

Supplemental Figure 4. Myeloid cells increase in the peripheral blood of IEC *C1galt1*$^{-/-}$ mice. (**A**) Peripheral leukocytes were stained with phycoerythrin-labeled mAbs to T cells (D90.2), B cells (B220), natural killer cells (NK1.1) and granulocytes (Ly-6G), as well as PerCP Cy5.5-anti-CD11b for myeloid cells). Neutrophils are Ly-6G^{+} CD11b^{+} (R3). Monocytes are Ly-6G^{-}CD11b^{+} (R2). (**B**) Monocytes (R2) were then identified as Ly-6C^{hi} or Ly-6C^{lo} subsets.

Supplemental Figure 5. Myd88 and TLR4 are dispensable in the pathogenesis of colitis in *O*-glycan–deficient mice. We bred IEC *C1galt1*$^{-/-}$ with mice lacking Myd88, an universal adaptor protein used by most TLRs, or TLR4, which recognizes bacterial antigens, and found that neither Myd88 nor TLR4 deficiency protected IEC *C1galt1*$^{-/-}$ mice from developing colitis. H&E-stained representative colonic sections indicate similar colonic inflammation in 20-week-old IEC *C1galt1*$^{-/-}$ mice with or without Myd88 or TLR4 deficiencies. Scale bar, 100 μm.

Supplemental Figure 6. Efficiency assessment of the depletion of gut microflora after NMVA treatment. (**A**) Aerobic and anaerobic bacterial colonies formed on sheep blood agar plates after inoculation of serially diluted stool from 12-week-old IEC *C1galt1*$^{-/-}$ mice with or without antibiotic treatment. The number at the center of each plate represents bacterial colonies. (**B**) Gram staining of stool samples from 12-week-old IEC *C1galt1*$^{-/-}$ mice with or without antibiotic treatment. Dark purple spots represent positive bacterial staining.

Supplemental Figure 7. Analysis of mRNA transcripts by real-time RT-PCR of different colonic mucins from WT colons and from TM-IEC *C1galt1*$^{-/-}$ colons before (0 d) and5 and 10 d after TM induction. Total RNA was extracted from colonic tissues and reverse transcribed into cDNA. β-actin and/or 18S RNAs were used as an internal control. Data are expressed as the fold difference between WT and TM-IEC *C1galt1*$^{-/-}$ mice (mean ± s.d., $n = 4$). The average mRNA levels in the colons of WT mice were expressed as 1.

Supplemental Figure 8. (**A**) Increased endocytosis of tight-junction protein, occludin, in the TM-IEC *C1galt1*$^{-/-}$ colonocytes compared to that of WT. Images of colon sections of 7-week-old WT and TM-IEC *C1galt1*$^{-/-}$ mice 5 d after TM induction stained with antibodies to occludin and F-actin. Arrows indicate internalized occludin. (**B**) The expression of ZO-1, another tight-junction protein, was unaltered in the TM-IEC *C1galt1*$^{-/-}$ colonocytes. Scale bar, 5 μm. Data are representative of two experiments.

Supplemental Figure 9. Loss of core 1 O-glycosylation does not causes unfolded protein and ER stress response (UPR). (**A**) Colon tissue cryosections of 12-wk-old WT and IEC *C1galt1*$^{-/-}$ mice stained with anti-Muc2 Gpda antiserum (PH497) that specifically recognizes non-O-glycosylated Muc 2 in the ER. Green color indicates positive staining of the Muc2 precursor. There was no significant accumulation of the Muc2 precursor in the IEC *C1galt1*$^{-/-}$ ER compared with the WT. Bars, 100 mm. (**B**) RT-PCR analysis of spliced and unspliced forms of XBP1 of total RNA isolated from WT (lanes 1

and 2) and TM-IEC *C1galt1*$^{-/-}$ (lanes 3 and 4) colons. Primers were designed to detect both unspliced (XBP1) and spliced XBP1. Spliced XBP1 indicates UPR. Mouse astrocytes treated with tunicamycin for 14 h, which inhibits N-linked glycosylation and causes UPR, were used as positive control (Lane 5). Untreated mouse astrocytes were used as negative control (lane 6).

Supplemental Figure 10. The expression of C3GnT is not altered in UC patient samples. Representative images showing that colon epithelial cells of patients with UC express a similar level of C3GnT (brown color) with that in the colon epithelia of normal controls. Scale bars, 50 μm.

Supplemental Figure 11. Tn-positive UC patient colon epithelium contains loss-of-function *C1GALT1C1* mutations. (**A**) *C1GALT1C1* exon 3 structure, which contains the entire open reading frame, locations of primers for mutation screening and *C1GALT1C1* PCR products of the Tn-positive and -negative epithelial cells of UC patients. (**B**) Direct sequencing results of PCR products from genomic DNA isolated from Tn-positive cells of an UC case showed both normal and mutated nucleotides of *C1GALT1C1* sequence at one location. (**C**) Sequence of the cloned PCR product from the same sample only has mutated nucleotide at position 677, confirming the mutation. (**D**) Schematic diagram of *C1GALT1C1* constructs. (**e**) RT-PCR showing that Jurkat cells stably expressed WT or mutant constructs, respectively. Lanes 1–5 represent Jurkat cells transfected with different *C1GALT1C1* constructs: 1, pcDNA3.1(vector only); 2, *C1GALT1C1* WT; 3, *C1GALT1C1* Mut I; 4, *C1GALT1C1* Mut III; 5, RNA without RT as a negative PCR control. (**f**) Flow cytometry analysis of Tn expression in Jurkat cells transfected with different *C1GALT1C1* constructs. For Tn staining, biotin-labeled mouse anti-Tn was used. Mouse IgM isotype was used as control. Bound anti-Tn was detected by FITC-streptavidin. Green line, Jurkat cells transfected with empty vector (pcDNA3.1) as control; filled line, *C1GALT1C1* WT; black line, *C1GALT1C1* Mut I; red line, *C1GALT1C1* Mut III.

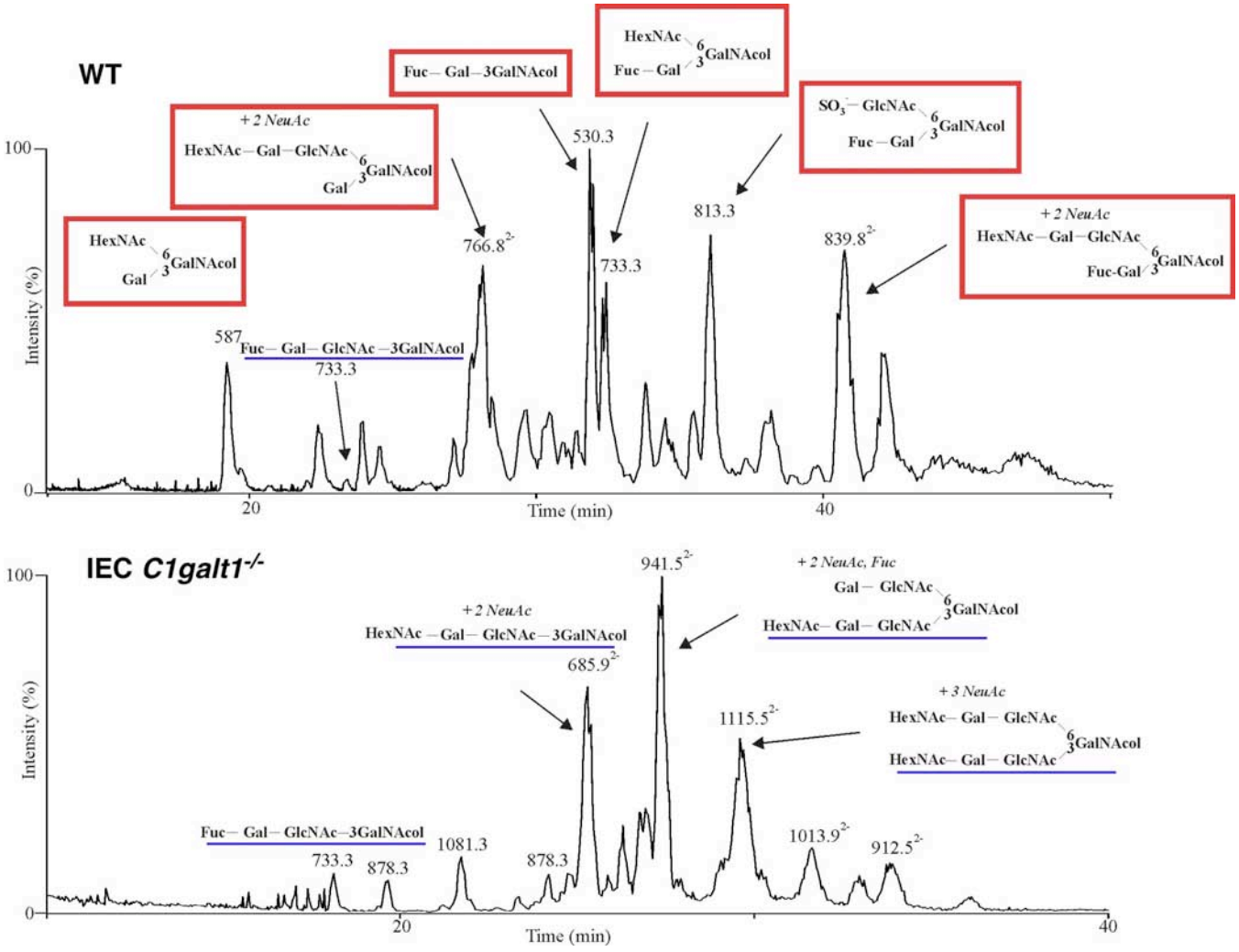

Supplemental Figure 1

Deletion of *C1galt1* abolishes the expression of core 1–derived *O*-glycans. Reversed-phase HPLC/mass spectrometry (LC-MS) profiling of Muc2 *O*-glycans purified from WT and IEC *C1galt1*$^{-/-}$ colon mucus. Red boxes indicate core 1–derived *O*-glycans, which were undetectable in the IEC *C1galt1*$^{-/-}$ colon sample. Blue lines mark core 3-derived *O*-glycans that were seen in both WT and IEC *C1galt1*$^{-/-}$ colon samples. Numbers represent calculated mass (*m*/*z*).

Accepted, J Clin Invest, Jan 10, 2010

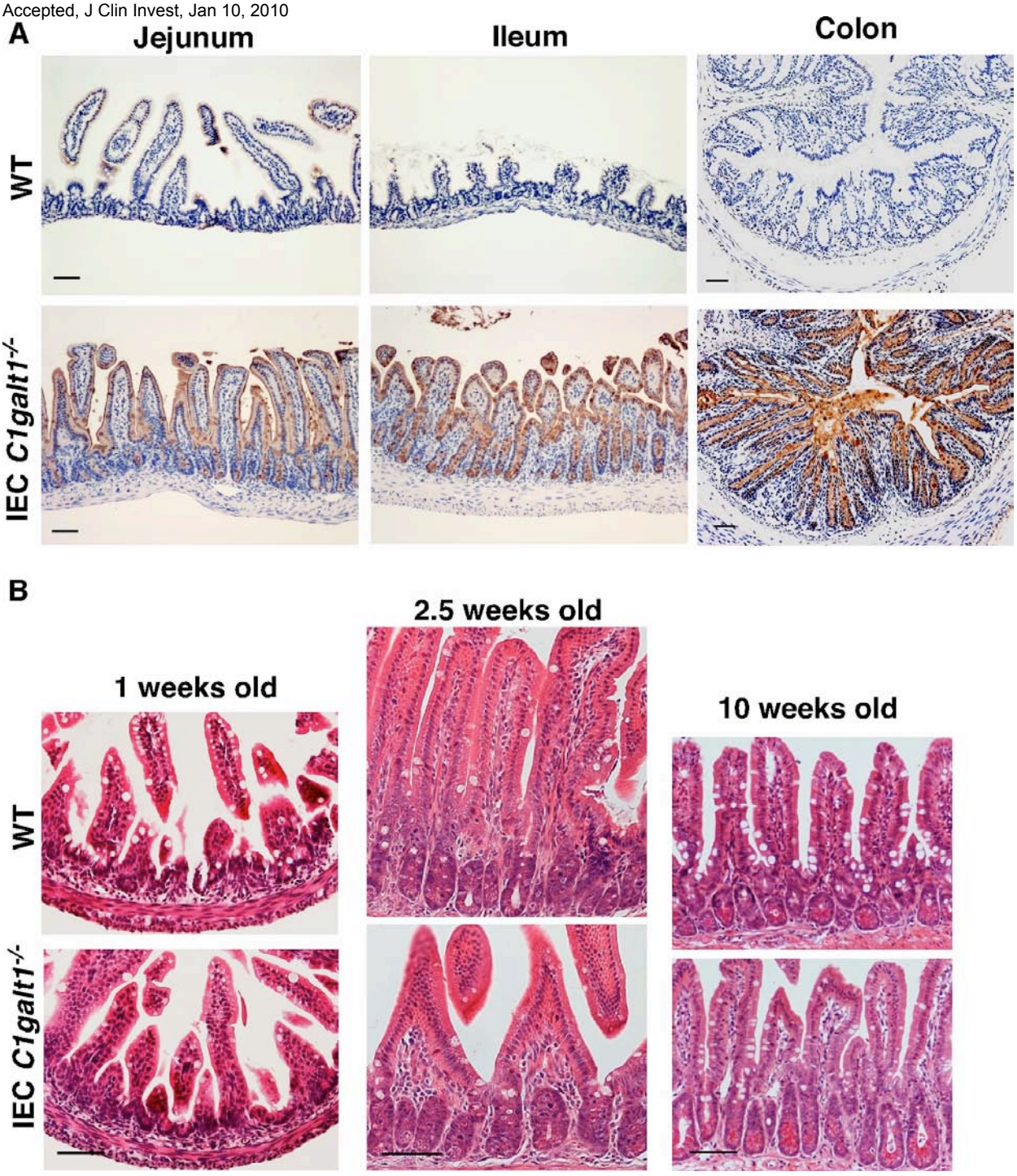

Supplemental Figure 2

IEC *C1galt1*$^{-/-}$ small intestine does not have significant inflammation. (**A**) Immunohistochemical staining of intestinal tissue sections of WT and IEC *C1galt1*$^{-/-}$ mice with anti–Tn antigen. Brown color indicates antibody binding. Scale bars, 100 μm. (**B**) H&E-stained WT and IEC *C1galt1*$^{-/-}$ ileums at different ages. Scale bars, 100 μm.

Accepted, J Clin Invest, Jan 10, 2010

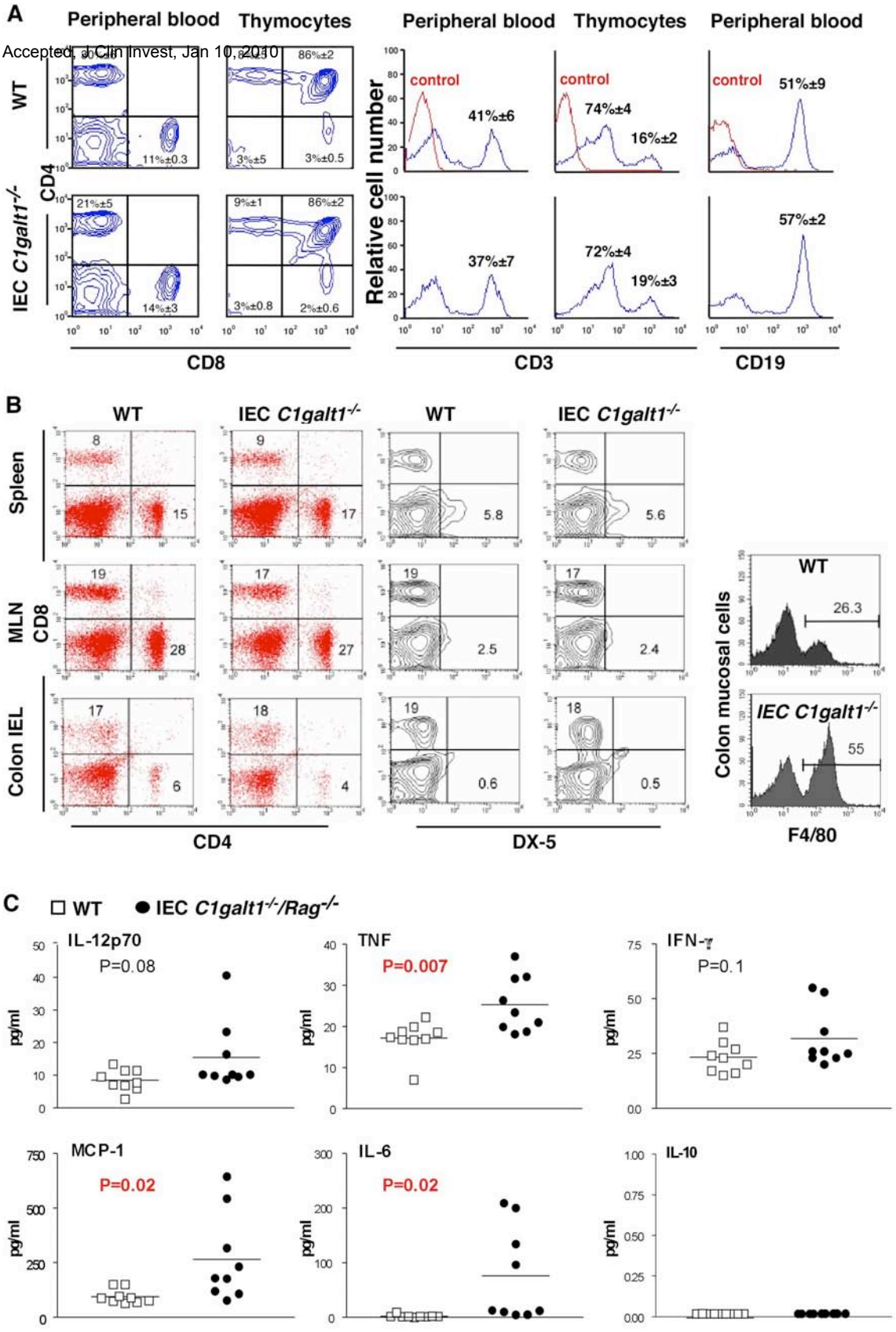

Supplemental Figure 3

Immune profiles of IEC *C1galt1*$^{-/-}$ mice. (**A**) Peripheral blood cell profiles of 4-week-old IEC *C1galt1*$^{-/-}$ mice. (**B**) Representative flow cytometry results of immune cells from different immune compartments of WT and IEC *C1galt1*$^{-/-}$ mice at 2.5 weeks old. IEL, intra-epithelial lymphocytes. CD4 and CD8, mAbs specific for these lymphocyte markers. DX-5, mAb specific for natural killer cells. F4/80, mAb specific for macrophages. (**C**) Serum cytokines of 2.5-week-old mice.

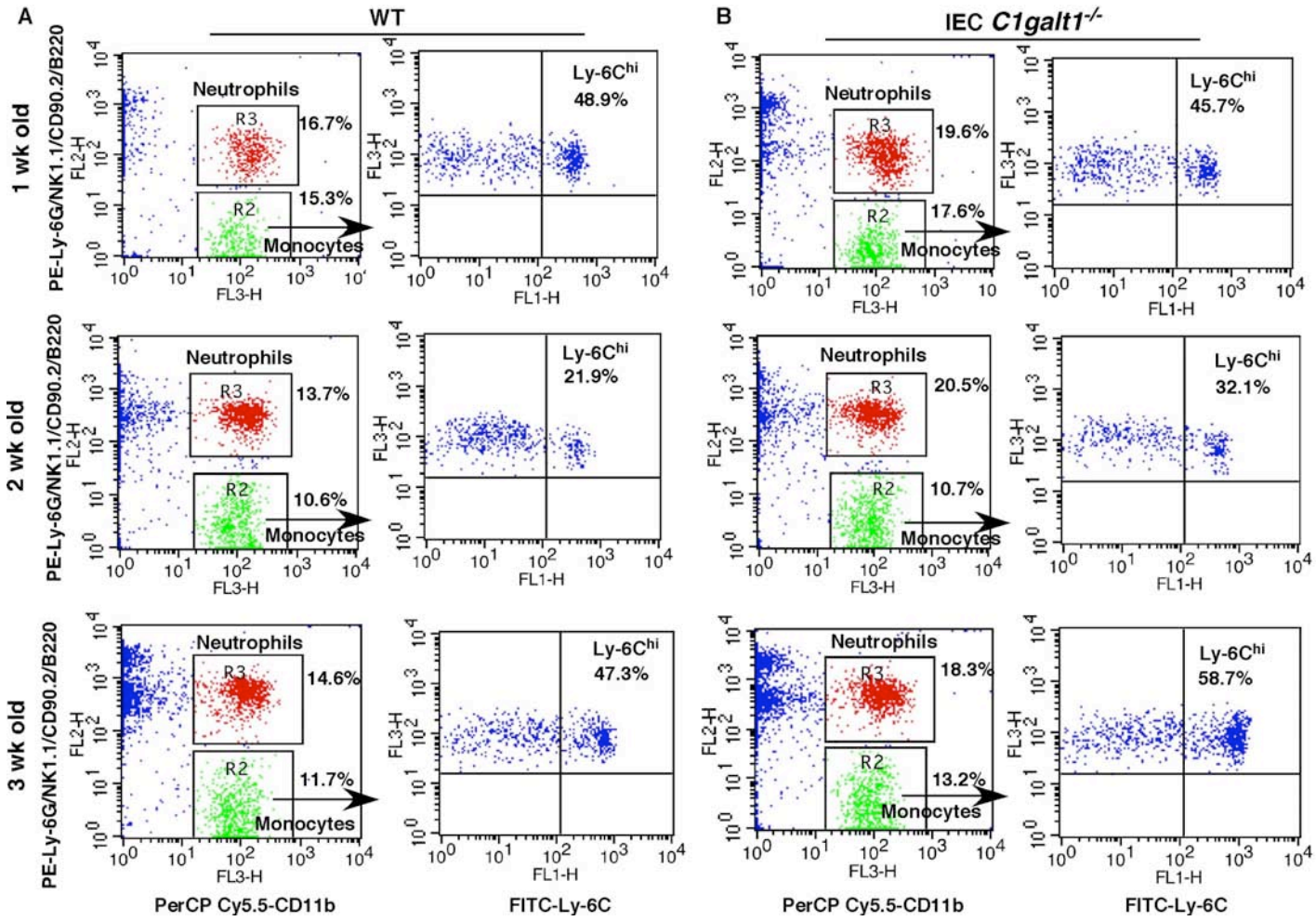

Supplemental Figure 4

Myeloid cells increase in the peripheral blood of IEC *C1galt1*$^{-/-}$ mice. (**A**) Peripheral leukocytes were stained with phycoerythrin-labeled mAbs to T cells (D90.2), B cells (B220), natural killer cells (NK1.1) and granulocytes (Ly-6G), as well as PerCP Cy5.5-anti-CD11b for myeloid cells). Neutrophils are Ly-6G^{+} CD11b^{+} (R3). Monocytes are Ly-6G^{-}CD11b^{+} (R2). (**B**) Monocytes (R2) were then identified as Ly-6C^{hi} or Ly-6C^{lo} subsets.

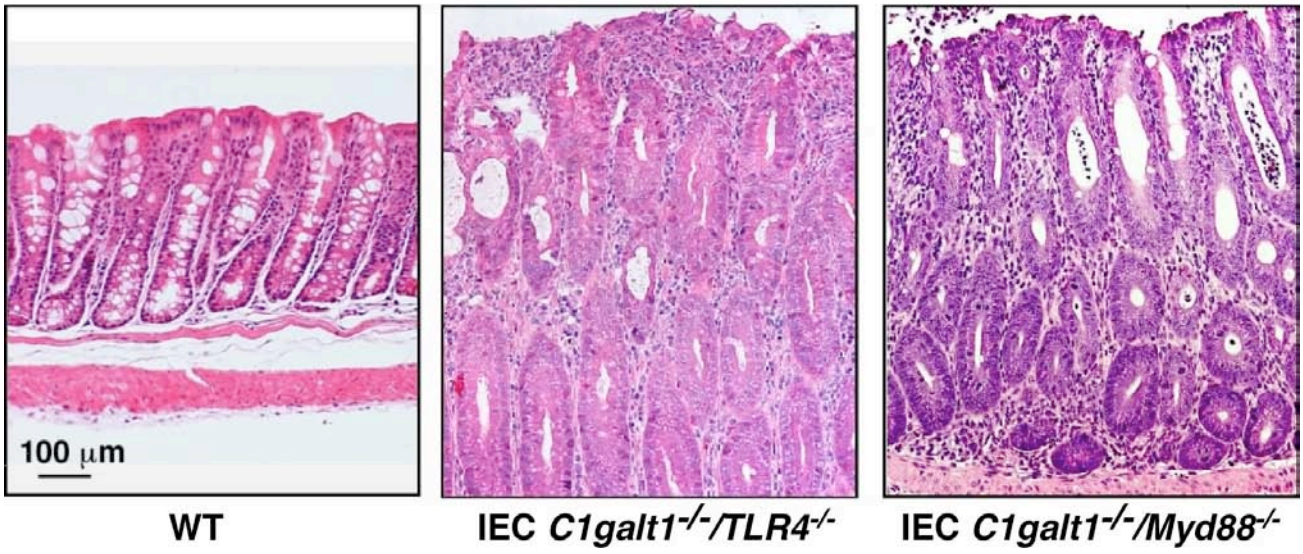

Supplemental Figure 5

Myd88 and TLR4 are dispensable in the pathogenesis of colitis in *O*-glycan–deficient mice. We bred IEC *C1galt1*$^{-/-}$ with mice lacking Myd88, an universal adaptor protein used by most TLRs, or TLR4, which recognizes bacterial antigens, and found that neither Myd88 nor TLR4 deficiency protected IEC *C1galt1*$^{-/-}$ mice from developing colitis. H&E-stained representative colonic sections indicate similar colonic inflammation in 20-week-old IEC *C1galt1*$^{-/-}$ mice with or without Myd88 or TLR4 deficiencies. Scale bar, 100 μm.

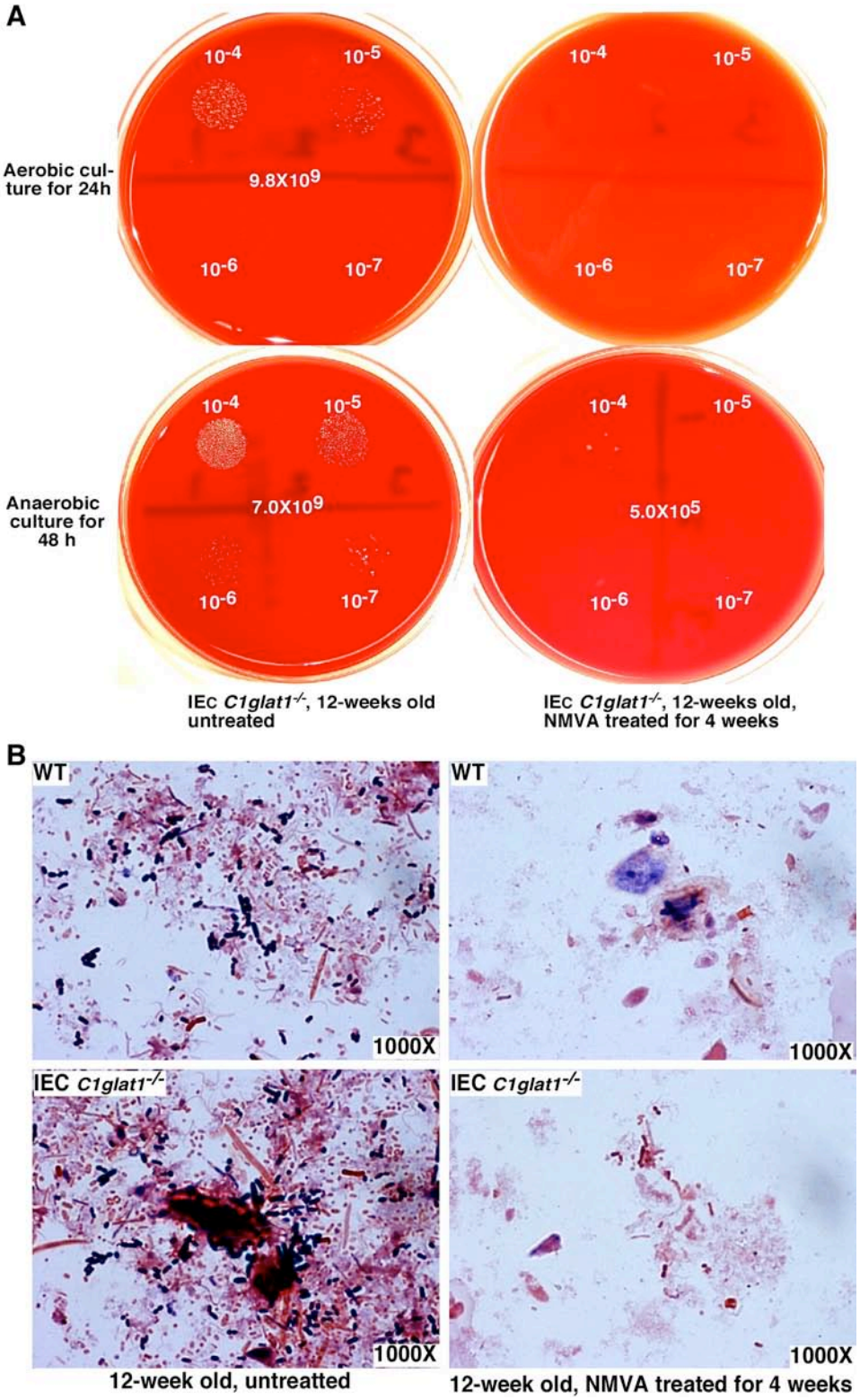

Supplemental Figure 6

Efficiency assessment of the depletion of gut microflora after NMVA treatment. (**A**) Aerobic and anaerobic bacterial colonies formed on sheep blood agar plates after inoculation of serially diluted stool from 12-week-old IEC *C1galt1*$^{-/-}$ mice with or without antibiotic treatment. The number at the center of each plate represents bacterial colonies. (**B**) Gram staining of stool samples from 12-week-old IEC *C1galt1*$^{-/-}$ mice with or without antibiotic treatment. Dark purple spots represent positive bacterial staining.

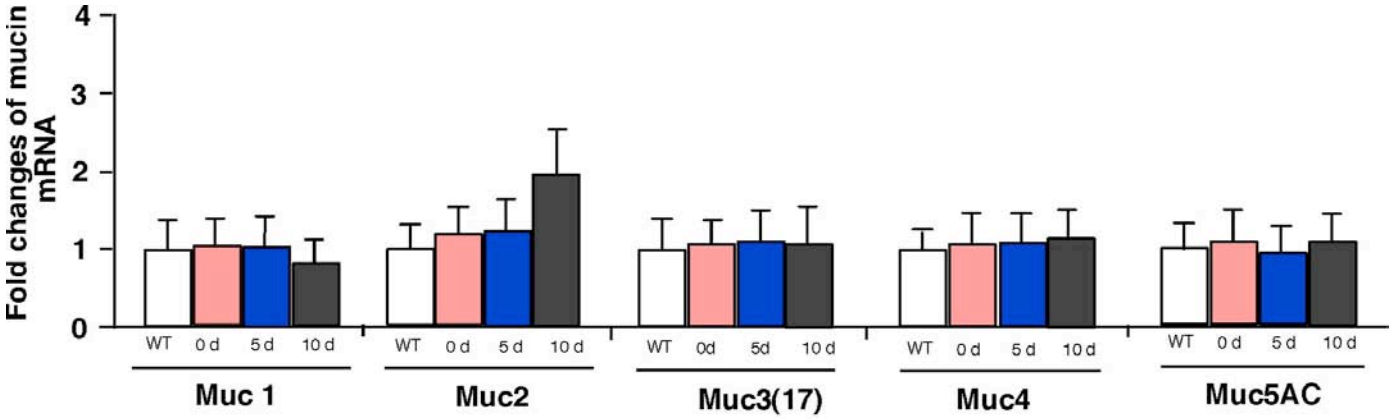

Supplemental Figure 7

Analysis of mRNA transcripts by real-time RT-PCR of different colonic mucins from WT colons and from TM-IEC *C1galt1*$^{-/-}$ colons before (0 d) and5 and 10 d after TM induction. Total RNA was extracted from colonic tissues and reverse transcribed into cDNA. β-actin and/or 18S RNAs were used as an internal control. Data are expressed as the fold difference between WT and TM-IEC *C1galt1*$^{-/-}$ mice (mean ± s.d., $n = 4$). The average mRNA levels in the colons of WT mice were expressed as 1.

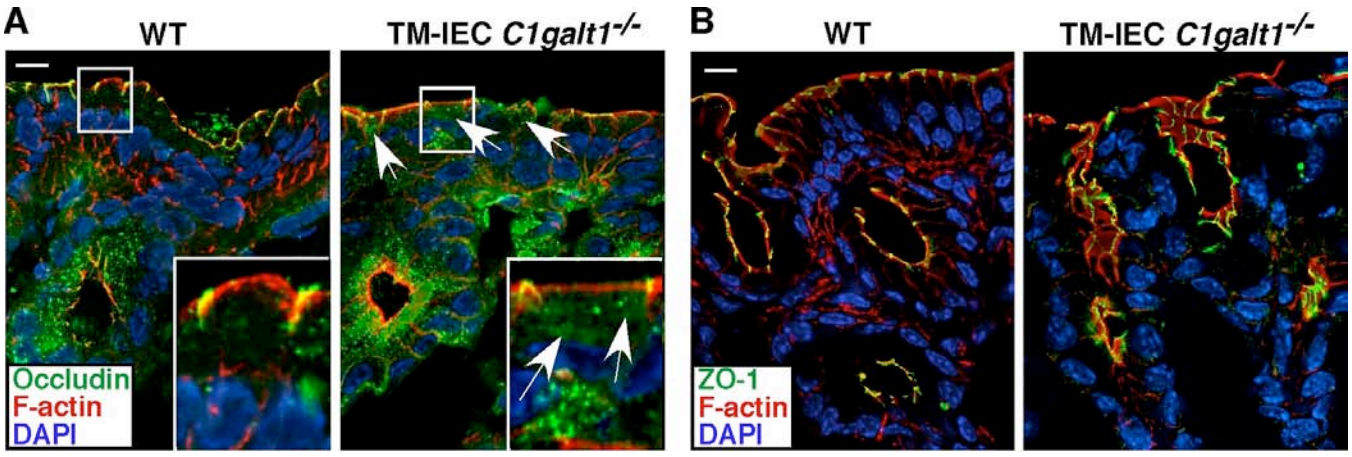

Supplemental Figure 8

(**A**) Increased endocytosis of tight-junction protein, occludin, in the TM-IEC *C1galt1*$^{-/-}$ colonocytes compared to that of WT. Images of colon sections of 7-week-old WT and TM-IEC *C1galt1*$^{-/-}$ mice 5 d after TM induction stained with antibodies to occludin and F-actin. Arrows indicate internalized occludin. (**B**) The expression of ZO-1, another tight-junction protein, was unaltered in the TM-IEC *C1galt1*$^{-/-}$ colonocytes. Scale bar, 5 □m. Data are representative of two experiments.

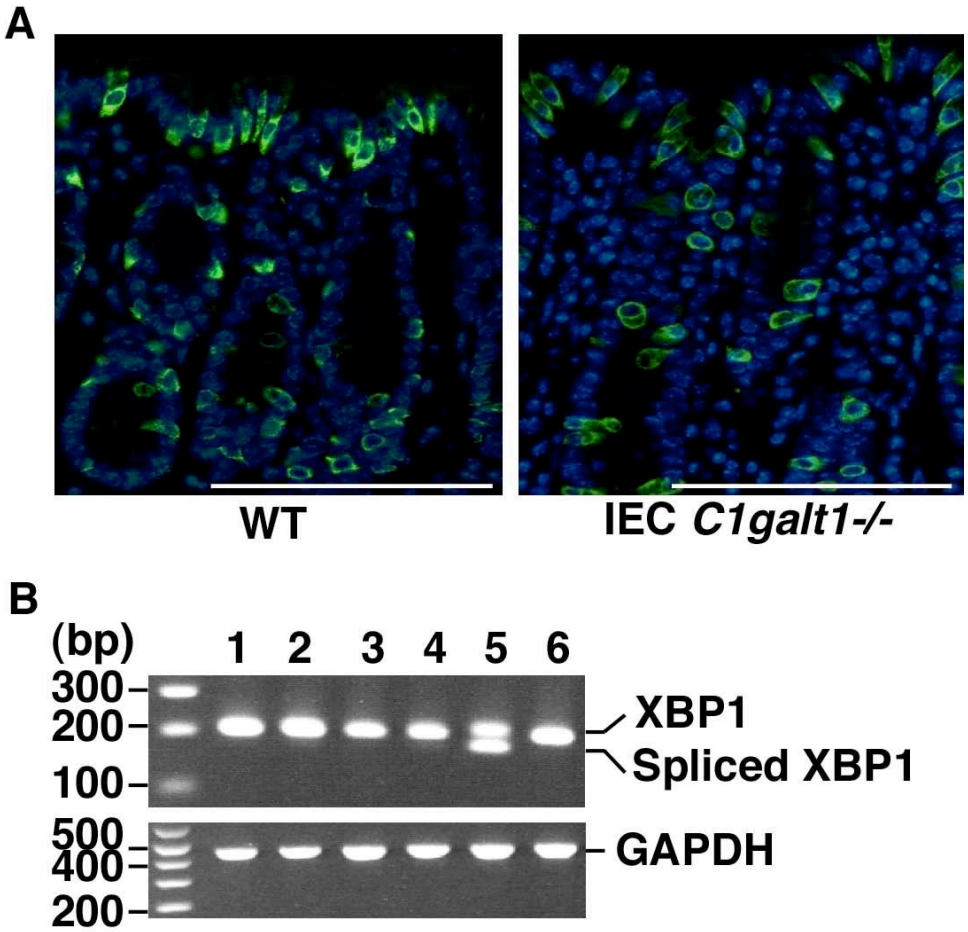

Supplemental Figure 9

Loss of core 1 O-glycosylation does not causes unfolded protein and ER stress response (UPR). (**A**) Colon tissue cryosections of 12-wk-old WT and IEC *C1galt1*$^{-/-}$ mice stained with anti-Muc2 Gpda antiserum (PH497) that specifically recognizes non-O-glycosylated Muc 2 in the ER. Green color indicates positive staining of the Muc 2 precursor. There was no significant accumulation of the Muc2 precursor in the IEC *C1galt1*$^{-/-}$ ER compared with the WT. Bars, 100 μm. (**B**) RT-PCR analysis of spliced and unspliced forms of XBP1 of total RNA isolated from WT (lanes 1 and 2) and TM-IEC *C1galt1*$^{-/-}$ (lanes 3 and 4) colons. Primers were designed to detect both unspliced (XBP1) and spliced XBP1. Spliced XBP1 indicates UPR. Mouse astrocytes treated with tunicamycin for 14 h, which inhibits N-linked glycosylation and causes UPR, were used as positive control (Lane 5). Untreated mouse astrocytes were used as negative control (lane 6).

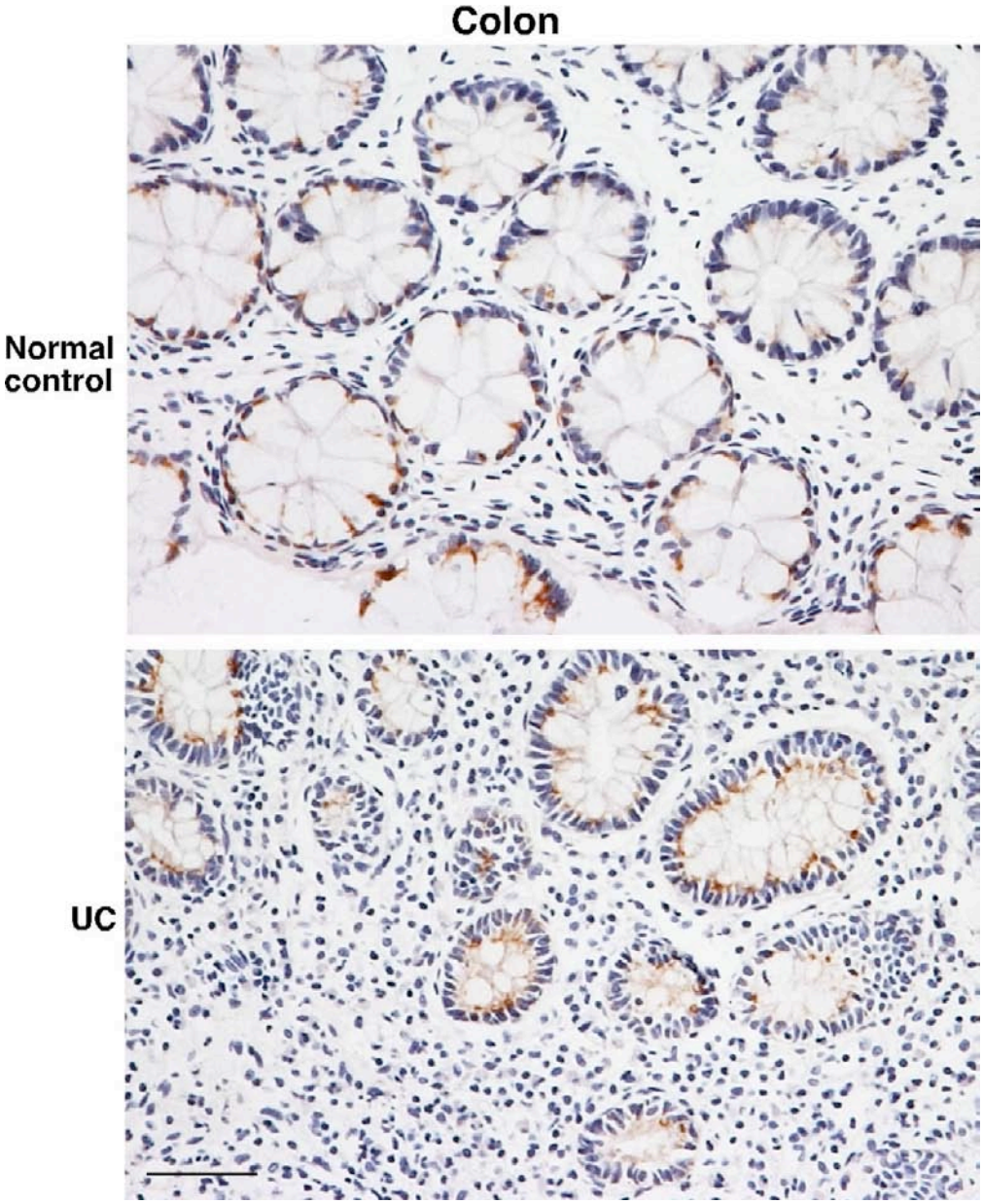

Supplemental Figure 10

The expression of C3GnT is not altered in UC patient samples. Representative images showing that colon epithelial cells of patients with UC express a similar level of C3GnT (brown color) with that in the colon epithelia of normal controls. Scale bars, 50 μm.

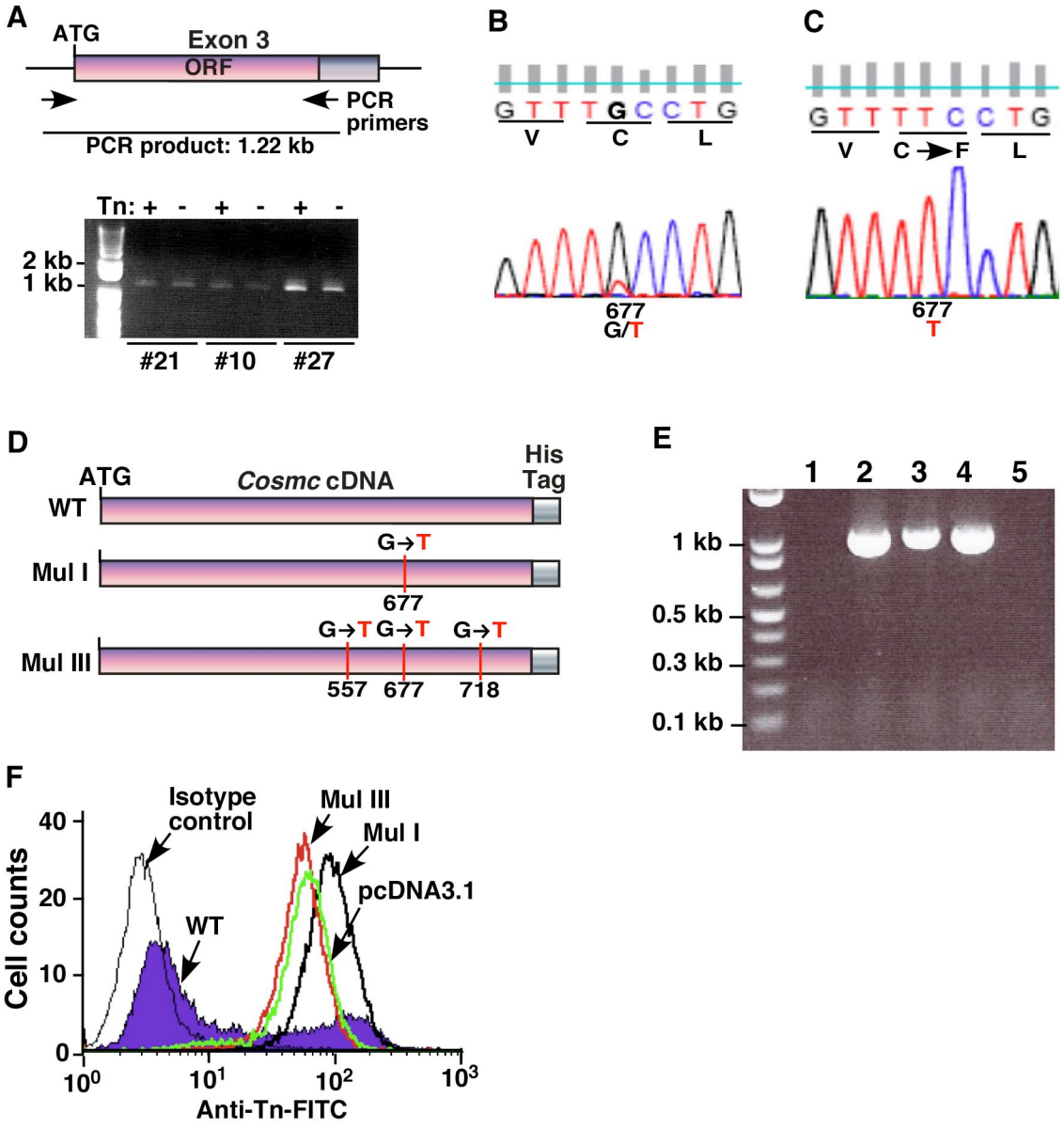

Supplemental Figure 11

Tn-positive UC patient colon epithelium contains loss-of-function *Cosmc* mutations. (**A**) *Cosmc* exon 3 structure, which contains the entire open reading frame, locations of primers for mutation screening and *Cosmc* PCR products of the Tn-positive and -negative epithelial cells of UC patients. (**B**) Direct sequencing results of PCR products from genomic DNA isolated from Tn-positive cells of an UC case showed both normal and mutated nucleotides of *Cosmc* sequence at one location. (**C**) Sequence of the cloned PCR product from the same sample only has mutated nucleotide at position 1205, confirming the mutation. (**D**) Schematic diagram of *Cosmc* constructs. (**e**) RT-PCR showing that Jurkat cells stably expressed WT or mutant constructs, respectively. Lanes 1–5 represent Jurkat cells transfected with different *Cosmc* constructs: 1, pcDNA3.1(vector only); 2, *Cosmc* WT; 3, *Cosmc* Mut I; 4, *Cosmc* Mut III; 5, RNA without RT as a negative PCR control. (**f**) Flow cytometry analysis of Tn expression in Jurkat cells transfected with different *Cosmc* constructs. For Tn staining, biotin-labeled mouse anti-Tn was used. Mouse IgM isotype was used as control. Bound anti-Tn was detected by FITC-streptavidin. Green line, Jurkat cells transfected with empty vector (pcDNA3.1) as control; filled line, *Cosmc* WT; black line, *Cosmc* Mut I; red line, *Cosmc* Mut III.